Chapter 2

Labels and Probes for Live Cell Imaging: Overview and Selection Guide

Scott A. Hilderbrand

Abstract

Fluorescence imaging is an important tool for molecular biology research. There is a wide array of fluorescent labels and activatable probes available for investigation of biochemical processes at a molecular level in living cells. Given the large number of potential imaging agents and numerous variables that can impact the utility of these fluorescent materials for imaging, selection of the appropriate probes can be a difficult task. In this report an overview of fluorescent imaging agents and details on their optical and physical properties that can impact their function are presented.

Key words: Fluorescence, fluorescent labels, fluorogenic probes, sensors, microscopy, imaging.

1. Introduction

Fluorescence imaging is a vital tool for the investigation of biological processes in the fields of cell, molecular, and systems biology. Its development has had a profound impact on our ability to decipher how these systems function at the cellular and molecular level. The development of fluorescence microscopy as an investigative tool has its origins in the 1850s with the first descriptions of "refrangible radiations" from biological materials by George Stokes (1). These radiations were later named fluorescence. However, the use of fluorescence as a diagnostic tool in microscopy would remain undeveloped until the construction of the first UV light microscopes by August Köhler in 1904 (2). Not long after the work of Köhler, the first purpose-built fluorescence microscopes were prepared, but it was not until the 1960s

D.B. Papkovsky (ed.), *Live Cell Imaging*, Methods in Molecular Biology 591,
DOI 10.1007/978-1-60761-404-3_2,

that these instruments became commonplace. Some of the first fluorescence microscopy experiments focused on observation of the intrinsic fluorescence of the biological samples under investigation (3). These investigations were invaluable for expanding our understanding of physiology, but they provided little insight on the function of biochemical and other physiological processes at a molecular level. For a more in depth investigation of these processes within the cell, a switch from intrinsic to extrinsic fluorophores is necessary. Today, numerous fluorescent materials are available for use in fluorescence microscopy.

Fluorescent compounds suitable for live cell imaging can be divided into two broad categories: labels and responsive probes. Fluorescent labels are imaging agents whose fluorescence signal remains constant. Good labels are typified by stable optical properties that do not vary significantly as a function of their local environment. These fluorescent species are often coupled with targeting groups or have genetically controlled expression. Responsive probes do not rely on preferential uptake or targeting. These sensors rely on changes in fluorescence intensity, wavelength, or lifetime for their function, and can be small molecule, polymer, or nanoparticle based. In this report we will provide an overview of current fluorescent labels and probes for use in live cell imaging of molecular processes.

2. Fluorescent Labels

The first advances toward the development of modern fluorescent labels are credited to the immunologist, Albert Coons in the 1940s. In his early research, he developed fluorescein isothiocyanate (FITC) (4), which remains one of the most ubiquitous fluorescent labels today, for coupling to antibodies targeted against pneumococcal bacteria. Today, targeted labels are among the most commonly employed fluorescent imaging agents. In addition to antibodies, targeting groups can be proteins, peptides, DNA aptamers, small molecule ligands, or stains for specific macromolecular structures. The emissive reporters in these labels can be fluorophores, fluorescent or bioluminescent proteins, or nanoparticles such as quantum dots. The efficacy of imaging with these compounds is dependent on their specific uptake, sequestration, or expression at a subcellular level.

2.1. Small Molecule Fluorophores

Prior to the development of FITC labels, a limited number of fluorophores with synthetic handles suitable for bioconjugation were available. Many of these early labels were based on dyes with fluorescence excitation in the UV (5). The fluorescence emission

signals from these dyes can be difficult to separate from tissue autofluorescence. In contrast, today there is a vast and often confusing array of fluorophore labels available to scientists. These fluorophores span the optical spectrum from the UV to the visible and extend into the near infrared (6–12). Many of the currently available amine reactive fluorophores are summarized in **Fig. 2.1 a**nd the structures of some representative labels are shown in **Fig. 2.2**. Several factors must be considered in choosing the appropriate fluorophores for constructing effective imaging agents. These include method of attachment to the targeting group, excitation and emission wavelengths, brightness, hydrophilicity, and cost.

There are many current chemistries available for the coupling of fluorescent labels to biomolecules and targeting groups (**Fig. 2.3**). The most frequently employed synthetic handle for bioconjugation is the succinimidyl ester, which forms stable amide bonds after reaction with primary and secondary amines. The isothiocyanate group may also be used for coupling to amines, generating a thiourea linkage. In cases where reaction of a succinimidyl ester or isothiocyanate derivatized fluorophore with an amine is not feasible, additional coupling groups are available. Iodoacetamide, maleimide, and dithiol-modified fluorophores are useful for covalent conjugation to thiols. Hydrazine and hydrazide modified dyes can be used for coupling to aldehydes and ketones, forming relatively stable hydrazone linkages. More recently, the development of bioorthogonal coupling schemes has attracted significant interest for preparation of fluorescent probes.

Bioorthogonal couplings rely on use of reaction partners that display little or no reactivity with common biological materials. Two examples of these reactions are the Staudinger ligation (13) and the "click" reaction (14). The Staudinger ligation involves coupling of a methyl ester electrophilic trap with an azide to generate an amide linkage and one equivalent of N_2. This reaction is mediated by oxidation of an adjacent phosphine. The click reaction is a copper(I) catalyzed [3+2] cycloaddition between an azide and an alkyne that results in the formation of a stable triazole product (14). This reaction has excellent potential for use in design of targeted fluorescent probes. However, there are only a few azide or alkyne modified dyes currently available for this reaction, most of which emit in the visible region. The potential utility of the click reaction in biology suggests that in the coming years the selection of azide and alkyne modified dyes is likely to expand greatly. For example, recent efforts have yielded new, efficient synthetic routes to far-red/near infrared emitting cyanine dyes modified with either azide or alkyne groups, one example of which, CyAM-5 alkyne, is shown in **Fig. 2.2** (15). Although highly selective, cytotoxic copper(I) is necessary for the traditional click coupling, and therefore direct use of this reaction in living biological systems has not been possible. The

Fluorophore	Abs (nm)	Em (nm)	ε ($cm^{-1}M^{-1}$)	ϕ_f	Ref.	Notes:
Dansyl chloride (DsCl)	337	492	5,300		6	*a*
Pyrenesulfonyl chloride	350	380	28,000		6	*b*
Coumarin-6-sulfonyl chloride	360	405			7	*c*
7-(Diethylamino)coumarin-3-carboxylic acid NHS	445	482			7	*d*
AF 350	346	445	19,000		6	*e*
AF 430	435	535	15,000		6	*e*
ATTO 390	390	475	24,000	0.90	8	*f*
ATTO 425	437	483	45,000	0.90	8	*f*
Dy 415	418	467	34,000		9	*g*

Fluorophore	Abs (nm)	Em (nm)	ε ($cm^{-1}M^{-1}$)	ϕ_f	Ref.	Notes:
NBD-X	466	535	22,000		6	*h*
FITC (5-isomer)	494	519	77,000		6	*i*
5-Carboxy-fluorescein	494	520	78,000		6	*i*
5(6)-Rhodamineisothiocyanate (TRITC)	544	572	84,000		6	*h*
Carboxy-tetramethylrhodamine (TAMRA)	554	584			7	*j*
Carboxy-X-rhodamine	575	605			7	*j*
AF 488	494	517	73,000	0.92	6	*e*
AF 546	554	570	112 ,000	0.79	6	*e*
AF 568	578	602	88,000	0.69	6	*e*
AF 594	590	617	92,000		6	*e*
AF 633	621	639	159,000		6	*h*
ATTO 488	498	520	90,000	0.80	8	*f*
ATTO 532	533	560	115,000	0.90	8	*f*
ATTO 550	554	574	120,000	0.80	8	*f*
ATTO 565	565	590	120,000	0.90	8	*f*
ATTO 590	594	624	120,000	0.80	8	*f*
ATTO 633	629	657	130,000	0.64	8	*f*
BODIPY FL	502	510	82,000		6	*h*
BODIPY TMR-X	544	570	60,000		6	*h*
Cy 3	548	562	150,000	0.04	10	*f*
Cy 3.5	581	596	130,000	0.14	10	*f*
Dy 495	493	521	70,000		9	*g*
Dy 547	557	574	150,000		9	*g*
Dy 590	580	599	120,000		9	*g*
Dy 610	610	630	80,000		9	*g*
Dy 631	637	658	200,000		9	*g*

Fluorophore	Abs (nm)	Em (nm)	ε ($cm^{-1}M^{-1}$)	ϕ_f	Ref.	Notes:
AF 647	651	672	270,000	0.33	6	*k*
AF 660	668	698	132,000	0.37	6	*k*
AF 680	684	707	183,000	0.36	6	*k*
AF 700	702	723	205,000	0.25	6	*k*
AF 750	753	782	290,000	0.12	6	*k*
ATTO 655	663	684	125,000	0.30	8	*f*
ATTO 680	680	700	125,000	0.30	8	*f*
ATTO 700	700	719	120,000	0.25	8	*f*
BODIPY 650/665-X	646	660	102,000		6	*h*
Cy 5	646	662	250,000	0.27	10	*f*
Cy 5.5	673	692	190,000	0.23	10	*f*
Cy 7	747	774	200,000	0.28	10	*f*
Dy 647	653	672	250,000		9	*g*
Dy 680	690	709	140,000		9	*g*
Dy 700	707	730	140,000		9	*g*
Dy 750	747	776	270,000		9	*g*
Dy 780	782	800	170,000		9	*g*
IRDye 800CW	774	789	240,000		11	*l*
IRDye 680	676	698	140,000		11	*l*
VivoTag 680	670	688	100,000		12	*f*
VivoTag-S 750	750	775	240,000		12	*f*

Notes: *a.* After reaction with alkylamine in CHCl3; *b.* after reaction with alkylamine in MeOH; *c.* after reaction with alkylamine in CH3CN; *d.* phosphate buffer, pH 7.0; *e.* aqueous, pH 7.0; f. aqueous; *g.* EtOH; h. MeOH; *i.* water pH 9; *j.* phosphate buffer, pH 8.0; *k.* quantum yield in PBS, pH 7.2, all other data in MeOH; *l.* PBS, pH 7.4.

Fig. 2.1. Commercial amine reactive fluorophore labels.

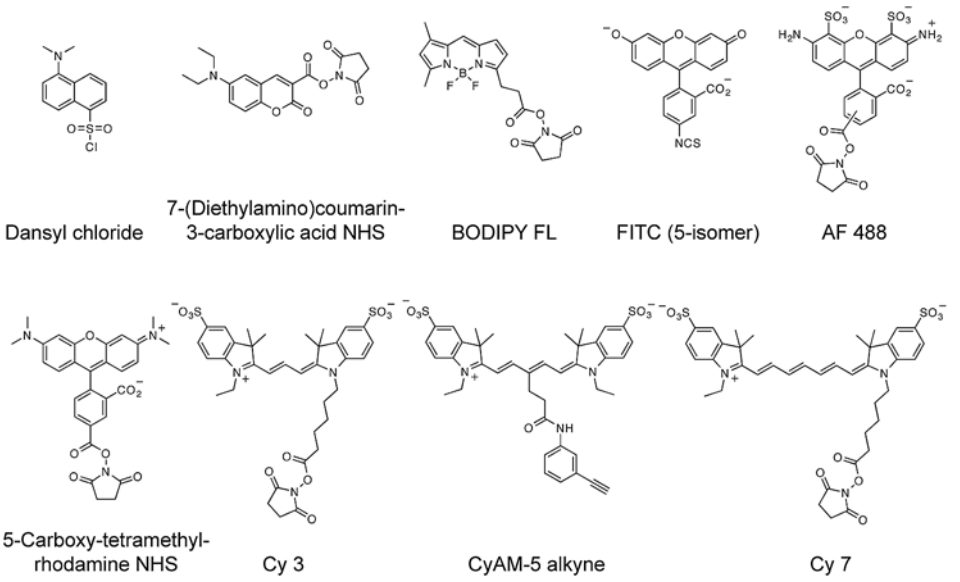

Fig. 2.2. Representative structures of fluorescent labels with emission in the blue (7-(diethylamino)coumarin-3-carboxylic acid NHS), green (BODIPY FL, FITC, and AF 488), orange (5-carboxy-tetramethylrhodamine NHS and Cy 3), far red (CyAM-5 alkyne), and near infrared (Cy 7).

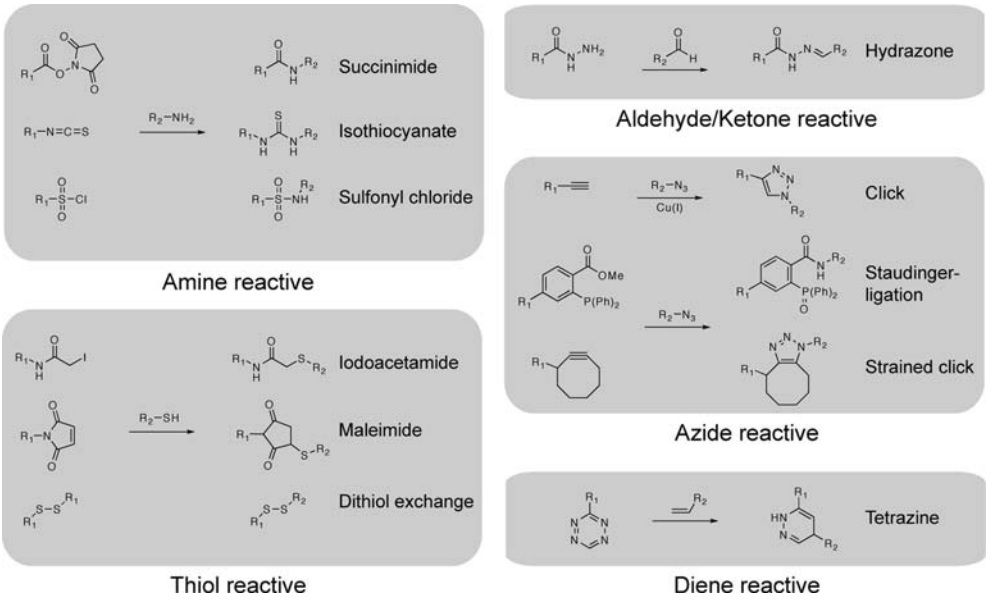

Fig. 2.3. Common coupling chemistries for attachment of fluorescent labels to targeting groups and biomolecules.

issue of copper cytotoxicity in the click reaction has been overcome by Bertozzi and others via preparation of new ring-strained cyclooctyne derivatives that do not require a catalyst (16–18). The coupling of cyclooctyne containing fluorophores with azide-modified sugars has been demonstrated for imaging

of surface glycosylation in live cells (16) and zebra fish embryos (19). Another bioorthogonal conjugation strategy compatible with live cells was reported in 2008 (20, 21). This coupling scheme involves use of an inverse-electron demand Diels–Alder cycloaddition between a modified tetrazine and a norbornene dienophile (20). The tetrazine-based coupling shows excellent selectivity in biological media and was used to label SKBR3 breast cancer cells that were pre-treated with norbornene modified trastuzumab (**Fig. 2.4**). The availability of labels for use with classical and bioorthogonal coupling reactions provides a wide selection of methods for attachment of fluorescent reporters to biological targets. The choice of coupling chemistry will be dependent on the specific reactive chemical groups available on the targeting molecule such as amines, thiols, or ketones. When the coupling or labeling reaction must be performed in a biological environment in the presence of live cells, the copper-free click reaction, Staudinger ligation, or the tetrazine cycloaddition reactions are appropriate conjugation methods.

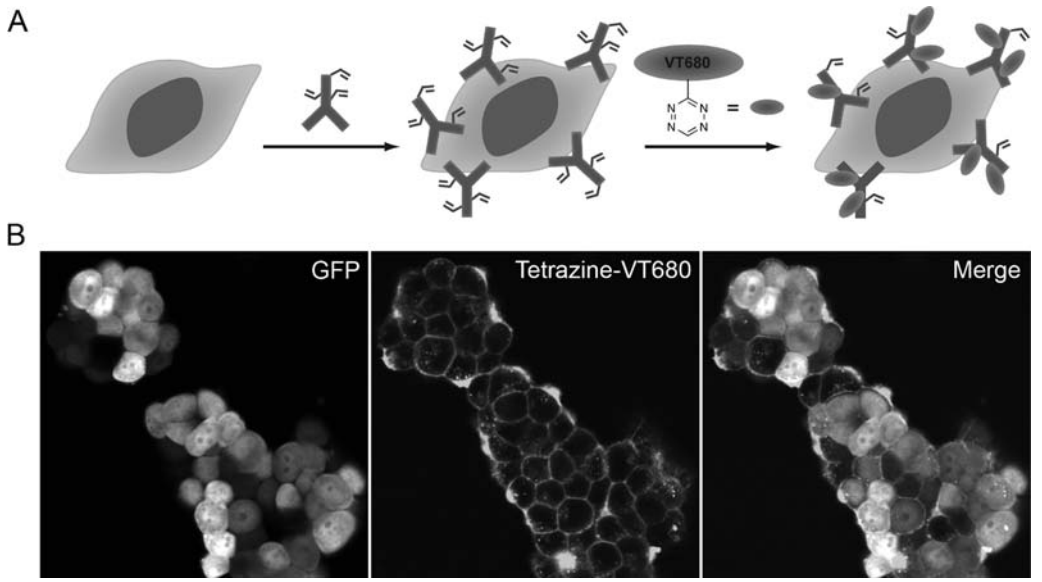

Fig. 2.4. Pre-targeting of GFP expressing SKBR3 human breast cancer cells with norbornene modified trastuzumab antibodies followed by addition of tetrazine-VT680, which covalently couples to the norbornene groups in an inverse electron demand Diels-Alder cycloaddition (**panel A**). **Panel B** shows confocal microscopy images of the cells after pre-targeting and VT-680 treatment in the GFP channel (*left*), VT680 channel (*center*), and the merged image (*right*).

Coupling chemistries have been used to prepare a wide array of imaging agents utilizing antibodies, aptamers, peptides, and small molecules. For example, anti-human epidermal growth factor 2 (HER2) antibodies conjugated with IRDye 800 were used to show antibody binding to HER2 expressing SKBR3 breast cancer cells and for in vivo fluorescence imaging in a mouse

model (22). DNA aptamers have also been used to target tumor cells (23). In much the same way, peptides have been coupled to a variety of fluorophores for preparation of several targeted imaging agents. This strategy has been widely used for targeting the $\alpha_v\beta_3$ integrin cell adhesion molecule with the RGD peptide motif for investigation of cancer cells and tissues (24–27). Targeting approaches need not be limited to short peptides. Larger peptides and proteins may also be used for directed delivery of optical reporters. Probes for selective imaging of epidermal growth factor receptor (EGFR) have been prepared via conjugation of Cy5.5 fluorophores to the 6-kDa epidermal growth factor protein. This probe was demonstrated to specifically home in on MDA-MB-468 cancer cells, which have high EGFR expression levels, but not to MDA-MB-435 cells which do not express EGFR (28). Small molecule based targeting strategies have also been employed through use of well-known bioactive small molecules such as folate (29) or through combinatorial approaches (30).

Peptide-based targeting has been expanded to incorporate bacteriophage nanoparticles as multivalent peptide carriers. This allows for facile integration of peptide screening for the cellular target of interest (via use of bacteriophage display libraries) with optical imaging and microscopy techniques. The M13 bacteriophage, commonly used in bacteriophage screening, has randomized peptide libraries displayed on its pIII coat proteins. The bacteriophage particles also contain 2700 copies of the pVIII coat protein, which have their amino termini exposed to the solvent. These amine groups are available for bioconjugation to fluorophores. Therefore, once a phage clone specific for the receptor of interest is identified, it can be modified via standard succinimide or isothiocyanate coupling procedures to prepare a fluorescent targeted imaging probe. This strategy was first demonstrated in 2004 (31) and further expanded for other imaging applications (32–34).

In addition to the bioconjugation strategy and selection of the targeting group, the optical properties of the fluorophore are another important factor in the design of targeted probes for live cell imaging. Although there are many fluorophores with excitation and emission in the UV, these fluorescent labels are not appropriate for certain imaging applications due to concerns regarding exposure of the cells to UV light, which may disrupt normal cell function. UV excitation may also result in higher background fluorescence signal from the sample, arising from the excitation of intrinsic biological fluorophores. Problems may occur with other common dyes, such fluorescein. Fluorescein is a pH-sensitive dye with a fluorogenic pK_a of 6.4; therefore, fluorescent labels containing fluorescein may display distinctly different fluorescence emission intensities depending upon the pH of their local environment. Consequently, for imaging

applications where the probe signal will be quantified, fluorescein may not be suitable. Other fluorophores with similar excitation and emission such as BODIPY FL or AF488 (6), which is based on a pH-insensitive rhodamine scaffold, are more appropriate for use in experiments requiring probe quantification. In many applications, labels with fluorescence emission in the NIR are preferred. NIR-emitting fluorophores are not susceptible to interference from biological autofluorescence and are directly translatable to many in vivo imaging applications due to the increased optical transparency of biological tissue between ~650 and 1000 nm (35). Fluorophores can show distinct changes in their fluorescence intensity and/or fluorescence emission wavelength based on the polarity of their local environment. The fluorescence quantum yields and emission wavelengths of dansyl fluorophores are well known to vary with the polarity of the surrounding media. Solvent polarity-based changes in fluorescence emission wavelengths and quantum yields can often be minimized by increasing the polarity of the fluorophore. Fluorophores that show little or no polarity-dependent changes on their optical properties tend to contain one or more solubilizing groups such as sulfonate or carboxylate moieties. For example, the optical properties of the near infrared emitting fluorophore, Cy5.5, which has four sulfonate groups, are relatively insensitive to changes in the local microenvironment.

Many fluorophores can be modified to act as optical switches that are activated by exposure to UV light. Several applications have made use of these photoactivatable or "caged" fluorophores. Caged fluorophores have been employed in dynamic imaging applications where specific temporal and spatial activation of a small population of fluorophore labels is required. These masked fluorophores, such as caged fluorescein, are prepared by reaction of the fluorophore with *o*-nitrobenzylbromide to form the non-fluorescent photoactivatable compound (36). The fluorescence can be activated by irradiation at 365 nm to cleave the *o*-nitrobenzyl group, releasing the free fluorophore (**Fig. 2.5**). In one early demonstration of this approach, microtubule flux in the mitotic spindle was monitored following photoactivation of caged fluorescein-labeled tubulin (36). Similarly, a caged resorufin was used to observe intracellular actin filament dynamics (37). More recently, a series of cell permeable caged coumarin derivatives (38, 39) has been designed for the study of intercellular gap junctions. After intracellular delivery of these caged fluorophores, a small population of the caged coumarins was activated and used as a fluorescent reporter to monitor the migration of the dye molecules through the gap junctions (39).

The brightness of the fluorophore is a key consideration. When targeting cellular components that are expressed in low levels, the fluorescence signal from the optical reporter needs to

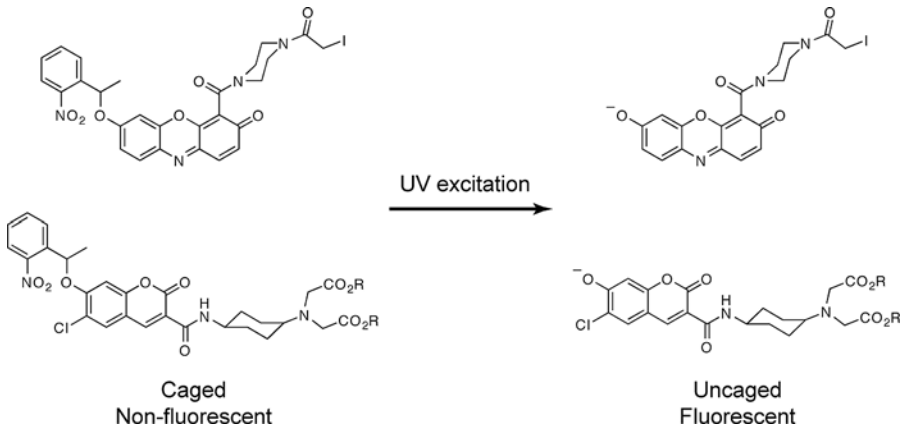

Fig. 2.5. Uncaging of non-fluorescent *o*-nitrobenzyl modified resorufin (*top*) and coumarin (*bottom*) derivatives after exposure to UV light.

be bright. The brightness is defined as the product of the fluorescence quantum yield and extinction coefficient of the fluorophore. For imaging low concentrations of cellular targets, weak fluorophores such as those based on NBD or pyrene may not be suitable. Some of the brightest fluorophores emitting in the visible are based on rhodamine or BODIPY scaffolds. Both of these fluorophore classes are typified by quantum yields approaching unity and extinction coefficients of 80,000 $M^{-1}cm^{-1}$ or more. In the far-red/NIR there are many bright fluorophores (6). Common NIR-emitting cyanine dyes are typified by large extinction coefficients often exceeding 200,000 $M^{-1}cm^{-1}$ and quantum yields of 20% or greater (10). However, the fluorescence quantum yields of fluorophores with emission > 800 nm begin to drop off considerably (34). This is the result of the relatively small energy difference between the ground and the excited states of these dyes, which allows for enhanced non-radiative decay of the fluorophore from the excited state.

The polarity of the fluorophore is an important factor in imaging agent design and may have a significant impact on the function of the fluorescent label. Many popular fluorescent labels are highly water-soluble polar species. Examples include AF488, fluorescein, sulforhodamine 101, and most cyanine-based far-red/NIR fluorophores. Imaging agents using polar fluorophores may not be able to cross the cell membrane by passive diffusion processes. Unless a targeted energy dependent transport mechanism is utilized, they are better suited for use as components of fluorescent reporters for imaging cell membrane or extracellular matrix components. Other fluorescent labels, such as DNA stains, rely on the permeability properties of the cell membrane for their function. These charged fluorescent molecules are often unable to penetrate healthy cells with intact membranes. If the membrane is compromised, as occurs with apoptotic or necrotic cells, these

dyes are able to enter the cell. One common method for preparing cell-permeable labels relies on the activity of intracellular esterases. The acetate or acetoxymethyl ester derivatives of many xanthene dye derivatives, such as fluorescein, are non-fluorescent, and non-polar, so that they may enter the cell via passive diffusion processes. Once inside the cell, the fluorescence signal of these fluorophores may be unmasked by intracellular esterase activity, which cleaves the acetyl groups from the fluorescein backbone, regenerating fluorescein. The free fluorescein is negatively charged under physiological conditions and therefore becomes trapped inside the cell (**Fig. 2.6**).

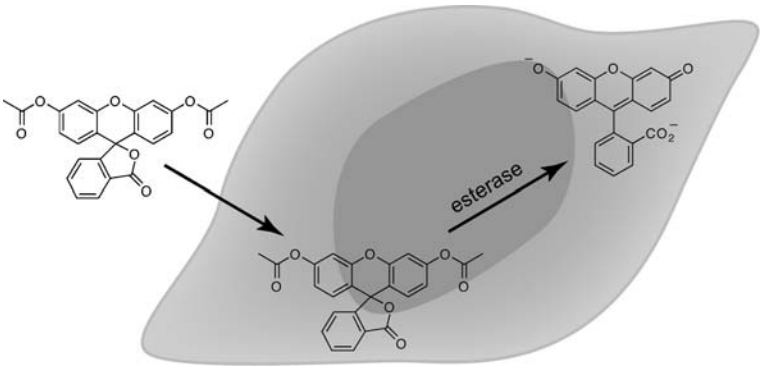

Fig. 2.6. Internalization of non-polar fluorescein diacetate followed by cleavage of the acetate groups by intracellular esterases, releasing polar fluorescein, which is trapped inside the cell.

Many of the more elaborate commercially available fluorophores are expensive, often costing over $200/mg. Certain imaging applications may require large quantities of probe, especially those involving in vivo microscopy. There are several more affordable fluorophore options with fluorescence emission in the visible range, such as fluorescein and rhodamine isothiocyanate derivatives (7). In contrast, there are few inexpensive commercially available NIR-emitting fluorophores, although efficient and inexpensive routes to prepare conjugatable fluorophores emitting in the NIR from commercially available precursors have been developed. The most common synthetic method is via nucleophilic attack on chloride containing carbocyanine precursors to install carboxylic acid functionality (34, 40, 41). These reactions can often be performed in a simple one-pot procedure with > 90% efficiency and do not require any purification step (34, 42).

2.2. Quantum Dot Labels

Luminescent semiconducting nanocrystals (QDs) are commonly used as labels for imaging at the cellular and subcellular levels (43 , 44). As with small molecule fluorophores, QDs have been

used for imaging a variety of cellular and subcellular targets. For example, targeting HER2 receptors on breast cancer cells and cytoplasmic actin and microtubule fibers has been demonstrated (44). Quantum dots are available with amine or carboxylic acid surface groups for bioconjugation reactions and come in a wide range of emission colors from the visible to NIR (6). Unlike organic dyes, quantum dots may be excited over a broad wavelength range with the highest extinction coefficients, often greater than 1,000,000 $M^{-1}cm^{-1}$, observed in the UV. These materials have several advantages over traditional fluorophores. The broad excitation range of QDs allows for simultaneous excitation of multiple quantum dots with different emission wavelengths using a single wavelength light source. Furthermore, QDs are not susceptible to rapid photobleaching under intense excitation, and therefore may be more suitable for confocal and other microscopy techniques, which require prolonged high intensity light exposure. Despite their significant advantages, QDs are not ideal for all imaging applications. Issues concerning QD blinking may complicate single molecule imaging experiments. Many quantum dots materials contain toxic cadmium (45), which was recently shown to leach out of the nanocrystal cores into the surrounding environment under certain biologically relevant conditions (46). In addition, commercially available QDs typically have a hydrodynamic diameter of 20–30 nm, significantly larger than small molecule organic fluorophores. The large size of the quantum dots may be a liability for imaging applications where the size of the fluorescent reporter could interfere with the function of the biological process under investigation. Actin fibers labeled with QDs have a proportionally decreased percent motility when compared to the corresponding AF488 organic fluorophore labeled filaments (47). Additionally, larger QDs may not be suited for monitoring fast diffusing neurotransmitters (48). As a result of their potential limitations for monitoring certain cellular processes, significant effort has been put forth to design improved quantum dots for live cell imaging applications. A large fraction of the typical QD diameter comes from polymer surface coating of the particles; therefore, efforts to decrease the thickness of this coating while maintaining ideal solubility characteristics could open QDs to new potential imaging applications. Following this strategy, QDs employing a short polyethylene glycol modified dihydrolipoic acid head group with a hydrodynamic diameter of 11 nm have been reported (49). Furthermore, the new smaller QDs have been engineered to contain only one site for biological labeling (49). Glutamate receptors labeled with the new, smaller QDs displayed a demonstrably improved ability to diffuse into neuronal synapses in comparison the corresponding commercial QD labeled receptors.

2.3. Genetically Encoded Labels

The researchers Roger Tsien, Martin Chalfie, and Samu Shimomura were recently awarded the 2008 Nobel prize in chemistry for their pioneering research on the identification, cloning, and modification of fluorescent proteins (50). Like QDs, genetically encoded fluorescent or chemiluminescent proteins are becoming commonplace. Recent reviews provide a comprehensive overview (51, 52). As with quantum dots and organic fluorophores, attention has been paid to developing fluorescent proteins in a rainbow of emission colors. Dozens of variants of these fluorescent proteins have been detailed in the literature (51), several of which are in use today with emission in the blue, green, yellow, orange, red, and far red from EGFP, EYFP, mOrange, mCherry, and mPlum, respectively. Unlike QDs and small molecule fluorophores, these species are useful in imaging applications where they can be used to monitor gene expression (53). Fluorescent proteins are also well suited for investigation of chemotaxis. Fluorescent protein expressing cells were used to investigate the role of the hematopoietic protein-1 (HEM-1) complex in cell motility (54, 55). The use of fluorescent proteins has been advantageous for the investigation of cell mitosis after challenge of human MDA cells with the anti-mitotic chemotherapeutics docetaxel (56) and paclitaxel (57).

Bioluminescent enzymes, like fluorescent proteins, are genetically encoded labels, although they require an additional substrate to generate a luminescent signal. Bioluminescent proteins have been isolated from a variety of organisms such as *Photinus pyralis* (firefly) (58), *Renilla reniformis* (sea pansy) (59), and *Pyrophorus plagiophthalamus* (click beetle) (60,61) with emission at ~480, ~560, and ~600 nm, respectively. The firefly and click beetle luciferases use luciferin, whereas the sea pansy luciferase requires colenterazine as a substrate. The lux operon may be used to investigate bacterial systems. This operon encodes both the luciferase and other proteins necessary for synthesis of the luciferin substrate (62, 63).

3. Responsive Probes

The use of targeted fluorescent labels and genetically encoded fluorophores has been invaluable in expanding our understanding of how the molecular machinery of the cell functions. However, these probes do not provide a detailed direct view of the function of many signaling molecules and messengers involved in cellular function. To investigate the interactions of these molecules, activatable or switchable smart probes are necessary.

The phenomenon of fluorescence is a particularly versatile process, with many different parameters that can be utilized for development of activatable probes. These properties include fluorescence intensity shifts, wavelength shifts, chemiluminescence activation, and fluorescence lifetime changes. Of these photophysical properties, most often biochemical probes are based on strategies to develop turn-on or wavelength-shift probes. Optimized fluorogenic probes share many selection criteria with targeted fluorescent labels. Factors to consider include biocompatibility and water solubility of the probes, suitability for extracellular or intracellular delivery, brightness of the fluorophore, and fluorescence excitation and emission wavelengths. In addition to these variables, other circumstances may influence the choice of probe. For example, selectivity of the imaging agent for the enzyme or analyte of interest is an important consideration. It is typically quite difficult to design a fluorogenic probe that displays complete selectivity to the target of interest. Virtually every known probe displays at least some basal activation by competing analytes or enzymes. The magnitude and mode of the fluorescence response is another factor. Typically activatable probes displaying an increase in emission or shifts in the absorption or emission spectra are preferred. Many turn-off fluorescence based sensors have been designed, but these agents are more difficult to use for cell imaging due to complications arising from detecting fluorescence decreases by microscopy. Turn-on probes can often be designed to show extremely strong fluorescence activation, often over 100-fold, but may not be suitable for experiments where quantitative measurements are required. With an off–on fluorescence response, it is difficult to account for baseline fluorescence signal arising from the non-activated probe and variations in the local concentration of the imaging agent. When quantitative measurements are required, sensors with a ratiometric fluorescence response are preferred. These sensors are suitable for quantitative measurements of analyte concentration because they allow for determination of the fluorescence activation in a manner independent of the local probe concentration. In the following sections, an overview of current turn-on and wavelength-shift fluorescence-based probes for bioimaging will be presented.

3.1. Enzyme Activation

Many enzyme activatable probes are based on the well-known phenomenon of self-quenching by organic fluorophores when held in close proximity to each other. An early example of this strategy in a fluorogenic probe suitable for use with live cells is a NIR-emitting fluorescent sensor for cathepsin D activity (**Fig. 2.7**). Cathepsin D is an aspartic protease that is known to be overexpressed in breast cancer cells. The probe consists of a polylysine polymer backbone modified with polyethylene glycol (PEG) polymers on the lysine side chains to improve solubility of the probe.

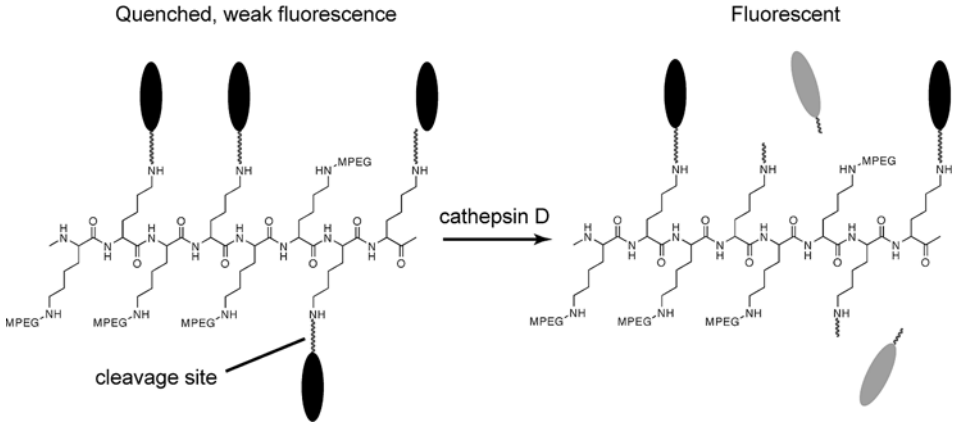

Fig. 2.7. Enzymatic activation of a polylysine based NIR activatable probe for cathepsin D.

In addition, several of the lysine side chains are further modified with a cathepsin D specific cleavage sequence containing NIR-emitting Cy5.5 fluorophores (64). Up to 24 Cy5.5 fluorophores are incorporated per polylysine polymer. The high density of fluorophores allows for efficient self-quenching of the dyes. In this case, more than 99% of the fluorescence emission of the Cy5.5 fluorophores is quenched in the probe (64). Upon cleavage of the probe with cathepsin D, up to 60-fold increase in fluorescence signal is possible. The effectiveness of this probe was demonstrated in vivo by imaging of mice bearing cathepsin D positive tumors where a signal-to-noise ratio of up to 22.8 was reported between tumor and non-target tissue (65). This flexible design strategy for enzyme activatable probes is useful for both endo- and exopeptidase enzymes. In addition to cathepsin D, fluorogenic probes for other enzymes such as cathepsin K, caspase-1, and MMP-2 utilizing this activation strategy have been reported (66–68).

An alternative strategy employed for the design of enzyme activatable probes does not rely on dye–dye quenching interactions. Instead, its fluorescence switching is based on chemical modification of the fluorophore reporter to alter its optical emission properties. One method for achieving this is by alterating the electronic structure of the fluorophore via formation of covalent bonds on portions of the fluorophore that are directly involved in fluorescence emission. For example, many classes of fluorophores such as 7-amino coumarins, rhodamines, fluoresceins, and Nile blue derivatives have amine or phenoxy groups that are part of their conjugated chromophore system and are available for chemical modification. Modification of these groups often has a dramatic effect on the fluorescence emission of the fluorophore. These changes are typified by strong hipsochromic shifts of the absorption maximum of the dye and a concomitant blue shift of

the emission maximum. In many cases, the quantum yield of the modified fluorophore is also significantly decreased. Enzyme activatable probes using this strategy can often show greater than 100-fold activation. This approach is useful for detection of enzymatic activity from exopeptidases. Many of these fluorogenic enzyme substrates have been prepared by conjugation of an amine group on 7-amino coumarin or rhodamine 110 to the carboxy terminus of a peptide sequence specific for the enzyme of interest. Formation of the amide bond on the coumarin or rhodamine abolishes the characteristic fluorescence emission at approximately 430 or 520 nm for the coumarin and rhodamine, respectively. Enzyme action on the substrate releases the coumarin and restores its fluorescent signal. A range of fluorogenic probes for peptidases activated by cathepsins (69), caspases (70, 71), elastases (72), and trypsin (72) have been developed using this approach. This strategy has also been adapted to fluorogenic probes for sugars and phosphatases (73).

3.2. Metal Ion Sensing

The design of effective probes for metal ions faces many challenges. The primary concerns are selectivity, metal ion affinity, and fluorescence response. There are numerous activatable and ratiometric fluorescence-based sensors for detection of bio-relevant ions such as Ca^{2+}, Mg^{2+}, Na^{2+}, K^{2+}, Zn^{2+}, Cu^{2+}, Fe^{3+}, and H^{+}. However, with the exception of pH responsive sensors (H^{+} ions), nearly every metal ion probe has side reactivity with analytes other than the targeted metal ion. Therefore the presence or absence of potential interfering ions influences the probe choice. The affinity of the analyte to the probe is another factor. The K_d values for analyte dissociation from the fluorescence-based sensor should be matched to the expected concentration of the ion under investigation to yield optimal response.

Fluorescent probes for calcium ions form one of the most diverse classes of metal ion sensors. The wide array of probes is in part due to the importance of calcium as a signaling molecule in biology. Cellular Ca^{2+} plays many functional and regulatory roles from muscle fiber contraction to signal transduction. Dozens of Ca^{2+} responsive sensors have been detailed in the literature, and a complete review of these probes is beyond the scope of this chapter. For more detailed information on Ca^{2+} probes, there are several excellent literature reviews (74, 75). Calcium ion probes can be divided into two broad categories: intensity based and ratiometric. Probes in both classes have a wide range of reported K_d values. For example, the fluorogenic Oregon Green 488 BAPTA-1, -6F, and -5 N probes, which are all based on the BAPTA (1,2-bis(*o*-aminophenoxy)ethane-*N,N,N′,N′*-tetraacetic acid) chelating group have tunable Ca^{2+} K_d values. By varying the substituents on the BAPTA chelator, the K_d for Ca^{2+} can be altered from 170 nM to 20 μM (**Fig. 2.8**) (6). Many low affinity

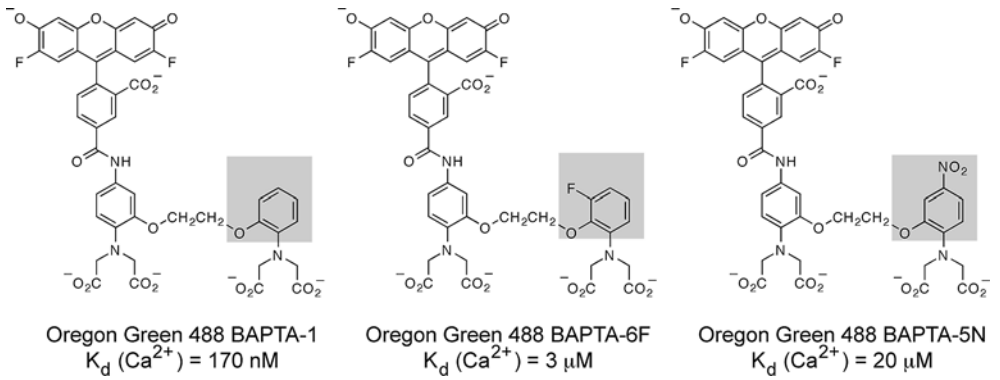

Fig. 2.8. Fluorogenic oregon green-based Ca^{2+} selective probes. The K_d values of these sensors can be tuned by altering the electron-withdrawing properties of the substituents on the BAPTA chelating moieties.

calcium binders also display selectivity for Mg^{2+}. The Mg^{2+} probe Mag-Fluo-4 has K_d values of 4.7 mM and 22 μM for Mg^{2+} and Ca^{2+}, respectively (6). The Mg^{2+} binding of this probe is well matched to the typical sub- to low-millimolar cellular magnesium levels (76). Ratiometric probes for Ca^{2+} can either show a change in absorption wavelength or emission wavelength upon coordination of the divalent ion. Examples include Fura-2 and Indo-1 for absorption and emission wavelength shift sensors, respectively (77). Ratiometric response with both classes of probes is possible, although sensors showing shifts in fluorescence emission are preferable since only one excitation source is necessary. This is particularly important in applications where laser excitation is used or where analysis will be performed by flow cytometry.

In addition to activatable probes for calcium, which were first reported in the early 1980s (78), recent years have seen the development of selective probes for many other metal ions. In the past decade significant attention has been directed toward imaging intracellular zinc to investigate its roles in biological homeostasis and signal transduction. Here we give an overview of several widely applied sensors for zinc. For a more complete survey of current Zn^{2+} selective probes, please see one of several recent reviews (79–81). Much of the pioneering work on design of efficient fluorescence-based zinc sensors originated in the Lippard and Nagano laboratories. The Lippard lab has reported a series of fluorescein-based probes for zinc using the dipicolylamine chelating group (82–85). The earliest of these probes, Zinpyr-1 displays a threefold increase in emission upon binding Zn^{2+} and has a 0.7 nM binding affinity (82). Sensors with decreased Zn^{2+} affinity have subsequently been prepared via replacement of one of the pyridyl arms of the dipicolylamine chelating motif with thiophene or thioether coordinating groups, decreasing the binding affinity

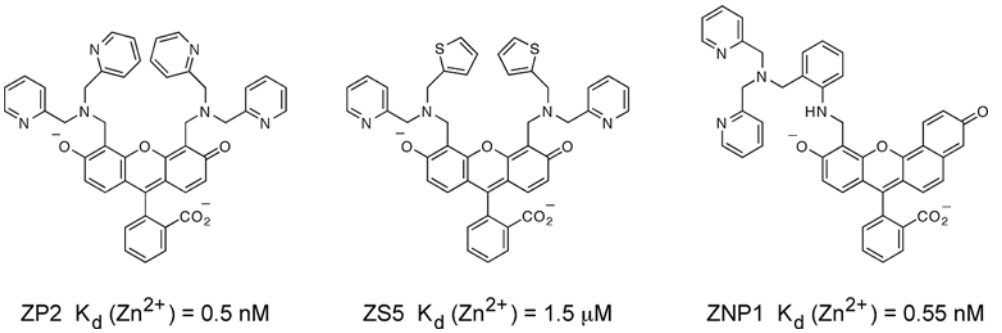

Fig. 2.9. Representative Zn^{2+} selective sensors. ZP2 and ZS5 are intensity based turn-on probes with sub nanomolar and micromolar Zn^{2+} affinities, respectively. ZNP1 is a ratiometric sensor with dual emission at 545 and 624 nm.

from the low nM to μM (**Fig. 2.9**) (86). One of these low-affinity probes, ZS5 was used to visualize glutamate-mediated Zn(II) uptake in dendrites and Zn(II) release resulting from nitrosative stress (86). As with Lippard, Nagano has focused on design of fluorescent Zn^{2+} sensors based on the fluorescein scaffold. Probes of the ZnAF family have low fluorescence background and strong activation of up to 69-fold upon Zn^{2+} coordination (87, 88). These sensors have been used to visualize Zn^{2+} release in the rat hippocampus (88) and to monitor presynaptic Zn^{2+} pools (89). Systematic modification of the dipicolylamine chelating moiety on these probes has enabled preparation of ZnAF probes with K_d values ranging from 2.7 nM to 600 μM (90). The ratiometric Zn^{2+} probes FuraZin and IndoZin, which are based on the related Fura and Indo Ca^{2+} sensors, (91) were used to monitor intracellular zinc uptake (92). Both FuraZin and IndoZin are excited at short wavelength (<400 nm) (91). To minimize potential phototoxic effects of UV excitation, long-wavelength ratiometric probes such as Zin-naphthopyr-1 (ZNP1), which has a 0.55 nM Zn^{2+} affinity, were designed (**Fig. 2.9**) (93). The ZNP1 probe has dual emission at 545 and 624 nm, where increasing [Zn^{2+}] induces a dramatic increase in the 624-nm emission signal. The diacetate derivative of this probe is membrane permeable and was used to image release of Zn^{2+} from COS-7 cells in real time (93). A NIR-emitting ratiometric probe, DIPCY, is based on a carbocyanine fluorophore scaffold (94) This probe, which has a Zn^{2+} K_d of 98 nM, displays an approximate 50 nm red-shift in its absorbance spectrum upon binding zinc.

Ion selective probes for H^+ are one of the oldest and most studied classes of ion sensors. Their development and use has been vital for investigation of pH changes in the endosomal/lysosomal system. Furthermore, disruption of acid/base homeostasis is associated with the pathophysiology of diseases such as cancer, cystic fibrosis, and immune dysfunction (95–98). Many fluorophores

have intrinsic pH sensitivity. For example, fluorescein has a fluorogenic pK_a of approximately 6.4 and has been used as a dual excitation single emission ratiometric probe for intracellular pH (99, 100). However, fluorescein can leak from cells and is used infrequently as a stand-alone probe for intracellular ratiometric pH imaging. New nanomaterials doped with FITC have been developed for ratiometric pH imaging. In one example, fluorescein and rhodamine isothiocyanate fluorophores (the rhodamine is used as a pH insensitive reference) were incorporated into core/shell silica nanoparticles and used for monitoring pH in intracellular compartments of mast cells (101). The dual excitation-single emission pH probe BCECF is one of the most widely used pH probes and is a fluorescein derivative modified with two carboxyethyl groups in the 2′ and 7′ positions of the dye. These additional carboxylate groups significantly improve intracellular retention of the sensor and contribute to an increase in the pH responsive pK_a to 6.97 (102). However, as a result of its dual excitation single-emission response, it is not ideal for imaging with laser microscopes or for flow cytometry experiments. To address this, single excitation dual emission pH responsive fluorophores were developed. In the early 1990s the seminaphthorhodafluor scaffold was designed for ratiometric pH imaging (103). In addition to having a single excitation dual emission response to pH with a pK_a of approximately 7.5, the probe exhibits red-shifted emission between 600 and 640 nm (103). One of these derivatives, carboxy-SNARF-1 has been used for imaging intracellular pH in chicken embryo epithelial cells (104). Probes for sensing pH can also be combined with targeting strategies. A series of pH responsive fluorogenic boron-dipyrromethene (BODIPY) fluorophores with tunable pK_a values between 3.8 and 6.0 were recently reported. These fluorophores can be conjugated to targeting groups such as trastuzumab for use as fluorescence-based switches and are activated by internalization into the endosomal/lysosomal system of cancer cells (105).

NIR fluorescent probes for pH sensing show potential for use in intracellular and in vivo pH measurement. Most current NIR pH probes are based on the carbocyanine scaffold. In one approach, dealkylation of one or both of the indole nitrogens on a non-pH responsive carbocyanine fluorophore renders it sensitive to pH (**Fig. 2.10**) (106–109). In contrast to xanthene based pH sensors, the carbocyanine dyes show an increase in fluorescence emission as the pH decreases. These probes have been used to monitor agonist-induced G protein-coupled receptor internalization into CHO or Hek293 cells (106). One pH responsive dye HCyC-646 with a fluorogenic pK_a of 6.2 and fluorescence emission at 670 nm was paired with pH insensitive Cy7 fluorophores on a bacteriophage particle scaffold for use as an nanoscale NIR ratiometric pH sensor (109). This system was used to monitor

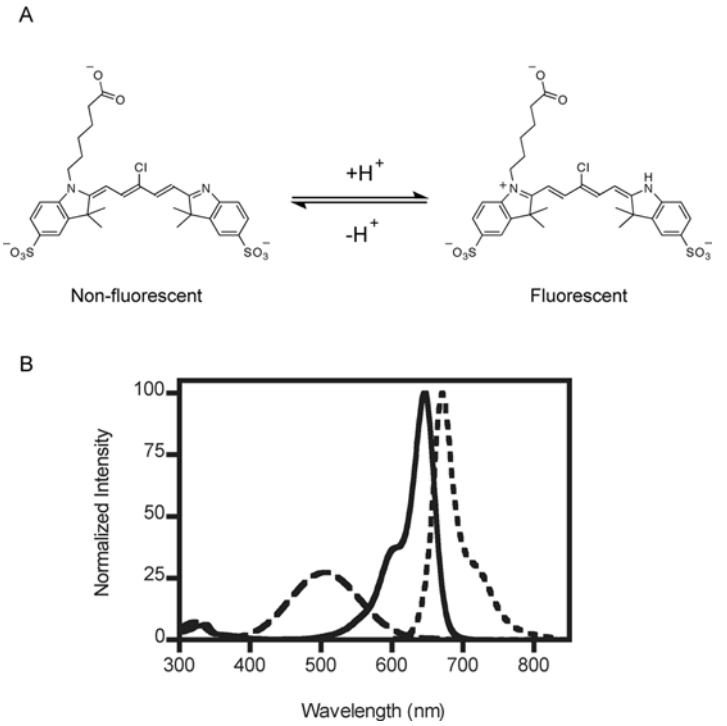

Fig. 2.10. The pH-dependent equilibrium showing activation of HCyC-646 at acidic pH (**panel A**). Absorption traces for HCyC-646 at pH 8 and pH 4 and fluorescence emission at pH 4, *dashed*, *solid*, and *dotted lines*, respectively (**panel B**).

intracellular pH following internalization into RAW cells and its potential for imaging pH in small animal models was demonstrated (109).

Although much recent work has focused on development of ion-selective probes specific for Ca^{2+}, Zn^{2+}, and H^+, many probes for other bio-relevant analytes have been developed. Ratiometric fluorescent indicators based different-sized crown ether ion chelators have been reported for Na^+ (SBFI, K_d = 3.8 mM) (110) and K^+ (PBFI, K_d = 5.1 mM) (110, 111), although they have relatively poor ion selectivity. Due to the potential role of unregulated cellular copper, in various diseases from amyotrophic lateral sclerosis (112) to Alzheimer's disease (113), fluorogenic copper specific probes have been designed (114–116). Additional efforts have focused on preparation of iron selective probes, but only a few turn-on sensors have been reported (117–120) and their ability for live cell imaging remains relatively untested.

3.3. ROS Sensing

There is significant interest in detection of reactive oxygen (ROS) and reactive nitrogen species (RNS) in biology. These reactive compounds are involved in multiple signal transduction and

regulatory processes. Furthermore, many of these compounds are strong oxidants and play critical roles in host defense and, when unregulated, in disease progression. One of the key challenges is the development of sensors with a high degree of specificity for a single analyte. This is often difficult since many of these species exhibit similar behavior as oxidants. Without selective sensors, it is very difficult to study the function of a single ROS/RNS since many different species are present simultaneously in the same biological systems. The inability to differentiate between specific reactive species has been the primary flaw of early probes such as 2′,7′-dichlorodihydrofluorescein (DCFH), which shows broad non-specific activation to a variety of oxidant species (121). In addition to this lack of selectivity, DCFH displays marked autoxidation activity when exposed to light.

Nitric oxide (NO) is one of the first reactive species for which selective fluorogenic sensors were developed. There are many approaches to imaging NO, and a more complete summary is given elsewhere (122, 123). The most common strategy today for design of selective NO sensors is based on the *o*-phenylenediamine functional group. In the presence of dioxygen and NO, a selective reaction occurs to convert the *o*-diamine into a triazole derivative (**Fig. 2.11a**). This effectively results in an increase in fluorescence signal since the amine groups of the *o*-phenylenediamine group, which are good photoinduced electron transfer (PET) quenchers, are converted into an electron deficient triazole. This approach has been used for design of a variety of NO sensors using naphthalene (124), fluorescein (125), BODIPY (126), rhodamine (127), and carbocyanine (128) fluorophores spanning the electromagnetic spectrum from the blue to NIR. In general, these probes show excellent selectivity for NO in aerobic environments with little or no observed reactivity to other oxidants such as peroxynitrite ($ONOO^-$), hydrogen peroxide (H_2O_2), or superoxide radical (O_2^-) (125). Although useful in most imaging applications, these sensors do not directly monitor NO. Fluorogenic sensors for NO based on the *o*-phenylenediamine functional group only react with RNS formed by the pre reaction of NO with O_2. Therefore detection is dependent not only on the presence of NO but also local O_2 levels.

A preferred tactic is fluorogenic sensors that are capable of direct reaction with NO. Recently the first probes suitable for live cell imaging based on direct detection of NO were reported (129). These sensors consist of a Cu(II) complex with a modified fluorescein derivative bearing an 8-aminoquinaldine chelating group (130). The paramagnetic properties of the Cu(II) coordinated to the fluorescein probe result in quenched fluorescence emission in the absence of NO. Reaction of this probe, CuFL, with NO results in reduction of the Cu(II) to Cu(I),

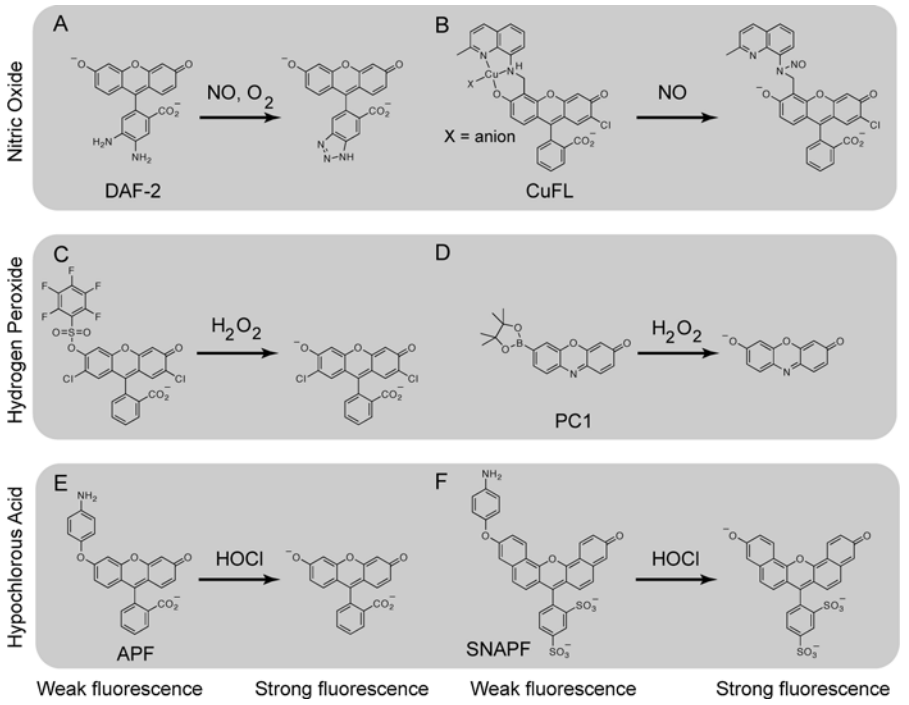

Fig. 2.11. Several examples of intensity based activatable sensors for nitric oxide, hydrogen peroxide, and hypochlorous acid.

release of the Cu(I) ion, formation of a nitrosamine modified fluorophore, and a strong increase in fluorescence emission (**Fig. 2.11b**) (130). CuFL shows a greater than tenfold increase in fluorescence upon combination with NO and like the *o*-phenylenediamine based probes has excellent selectivity, with minimal side reactivity to $ONOO^-$ (130).

There are many approaches for development of selective probes for H_2O_2. One strategy relies on the cleavage of sulfonate-protected fluorescein (**Fig. 2.11c**) (131, 132) or naphthofluorescein (133) scaffolds. However, these probes typically have non-trivial side reactivity with several oxidants such as O_2^-, $OH^{\cdot}$, or hypochlorous acid (HOCl) (131, 133). In an alternative approach, chemospecific probes for H_2O_2 have been reported based on the specific chemical reaction of H_2O_2 with boronate esters to give phenol species (**Fig. 2.11d**) (134). This detection strategy has been used to prepare fluorogenic xanthene and resorufin derivatives with either one or two reactive boronate esters (134–136). As a result of their non-polar composition, the sensors have innate cell permeability and depending on the fluorophore scaffold emit in the blue (135), green (134, 136), or red (135–137). The boronate ester-based H_2O_2 sensors show a dramatic fluorescence response; in the case of the fluorescein-based probe PF1, a >500-fold increase in fluorescence signal is observed

upon reaction with H_2O_2 (134). The diboronate ester modified probes are somewhat less sensitive than the monoboronate modified probes and are more suitable for monitoring H_2O_2 under conditions of oxidative stress. The more sensitive monoboronate modified sensors PG1 and PC1 were used recently to visualize physiological signaling concentrations of H_2O_2 in live cells (136). In addition to the more common fluorescence based signaling mechanisms, a selective chemiluminescence based H_2O_2 detection scheme has been reported (138). In this system, a chemoselective reaction occurs between H_2O_2 and peroxylate ester polymeric nanoparticles generating high-energy dioxetanedione intermediates, which in turn chemically excite polycyclic aromatic fluorophores embedded in the nanoparticles.

Hypochlorous acid is an important strong oxidant involved in host defense and has been implicated in the pathogenesis of several disease states. In biology, it is produced by the enzyme myeloperoxidase (MPO), which converts H_2O_2 and Cl^- ions into HOCl. Few probes have been developed that are capable of selective detection of this important cellular oxidant. The first reported sensor capable of efficient HOCl detection is aminophenyl fluorescein (APF) (121). APF shows excellent response to HOCl, generating fluorescein as a final oxidation product and displays several 100-fold fluorescence activation (**Fig. 2.11e**). However, it also shows significant cross reactivity with $ONOO^-$ and $OH^{\cdot}$ (121). This lack of specificity can be overcome when APF is used in conjunction with the chemically related HPF, which only reacts with $ONOO^-$ and $OH^{\cdot}$ (121). The selectivity of this system has been further tuned by careful selection of the fluorophore scaffold. Using the same *p*-aminophenylether reactive group, the sulfonaphthofluorescein based probe (SNAPF) displays enhanced ROS selectivity (**Fig. 2.11f**). SNAPF is activated exclusively by HOCl and has been used to monitor MPO generated HOCl in vitro, in cell culture, and in vivo (139). Although it does react specifically with HOCl, the SNAPF probe is still not ideal as it only shows an approximately tenfold fluorescence response when exposed to HOCl (139). Continued efforts in this field will undoubtedly yield improved probes for selective detection of HOCl.

In addition to efforts for preparation of selective probes for reactive small molecules such as NO, H_2O_2, and HOCl, sensors for several other species have been designed. Of these, there are few fluorogenic probes specific for $OH^{\cdot}$ or O_2^-. However, recently a new class of carbocyanine dyes, the hydrocyanines, has been reported that is sensitive to both superoxide and hydroxy radicals (140). These probes are prepared from conventional carbocyanine fluorophores via selective reduction. When the reduced carbocyanines are exposed to ROS, they are oxidized back to their parent carbocyanine fluorophore. Peroxynitrite responsive

probes have also been reported. These sensors only show a seven- to eightfold activation for $ONOO^-$ and have marked side reactivity with other ROS such as $OH^{\cdot}$, with an observed threefold activation (141). Nevertheless, there is promise for development of more selective peroxynitrite sensors based on this activation scheme. Although less active than the invesitgation of ROS or RNS, there is interest the bioimaging of thiols. Imaging of thiols can give insight into local redox status. Furthermore, the presence of thiol containing amino acids such as homocysteine have been associated with a variety of disease states (142, 143). To this end, there have been several recent reports of fluorogenic and ratiometric probes for thiol bioimaging (144–147).

4. Summary

There are many fluorescence-based imaging agents for biological targets, enzymes, and other analytes. Targeted fluorescent labels utilizing affinity groups from antibodies to small molecules have been developed and many activatable sensors for metal ions from calcium to zinc have been designed. In addition, there are several different classes of activatable imaging agents for the detection of enzyme activity and reactive small molecules. As a result of the large pool of potential imaging agent choices, it can often be difficult to select the most appropriate imaging agent for a particular experiment. The ability to identify an effective fluorescent reporter can be facilitated by careful consideration of factors such as the conjugation chemistry, photophysical characteristics, polarity, cost, and selectivity of the imaging agent.

References

1. Stokes, G. G. (1852) On the change of refrangibility of light. *Phil. Trans. R. Soc. London* **142**, 463–562.
2. Köhler, A. (1904) Mikrophotographische einrichtung: eine für ultraviolettes licht (λ = 275 nm) und damit angestellte untersuchungen organischer gewebe. *Phys. Z.* **5**, 666–673.
3. Stübel, H. (1911) Die fluoreszenz tierischer gewebe in ultraviolettem licht. *Pflug. Arch. Ges. Phys.* **142**, 1–14.
4. Coons, A. H., Creech, H. J., Jones, R. N., and Berliner, E. (1942) The demonstration of pneumococcal antigen in tissues by the use of fluorescent antibody. *J. Immunol.* **45**, 159–170.
5. Coons, A. H., Creech, H. J., and Jones, R. N. (1941) Immunological properties of an antibody containing a fluroescent group. *Proc. Soc. Exp. Biol. Med.* **47**, 200–202.
6. Molecular Probes Inc., Eugene, OR: http://probes.invitrogen.com.
7. Sigma-Aldrich Corp., St. Louis, MO: http://sigmaaldrich.com.
8. ATTO-TEC GmbH, Siegen, Germany: http://atto-tec.com.
9. Dyomics Gmb H, Jena, Germany: http://www.dyomics.com.
10. GE Healthcare Bio-Sciences Corp., Piscataway, NJ: http://www.gelifesciences.com.
11. LI-COR Biosciences, Lincoln, NE: http://www.licor.com.

12. VisEn Medical Inc., Woburn, MA: http://www.visenmedical.com.
13. Chang, P. V., Prescher, J. A., Hangauer, M. J., and Bertozzi, C. R. (2007) Imaging cell surface glycans with bioorthogonal chemical reporters. *J. Am. Chem. Soc.* **129**, 8400–8401.
14. Rostovtsev, V. V., Green, L. G., Fokin, V. V., and Sharpless, K. B. (2002) A stepwise Husigen cycloaddition process: copper(I)-catalyzed regioselective "ligation" of azides and terminal alkynes. *Angew. Chem., Int. Ed.* **41**, 2596–2599.
15. Shao, F., Weissleder, R., and Hilderbrand, S. A. (2008) Monofunctional carbocyanine dyes for bio- and bioorthogonal conjugation. *Bioconjug. Chem.* **19**, 2487–2491.
16. Baskin, J. M., Prescher, J. A., Laughlin, S. T., Agard, N. J., Chang, P. V., Miller, I. A., Lo, A., Codelli, J. A., and Bertozzi, C. R. (2007) Copper-free click chemistry for dynamic in vivo imaging. *Proc. Natl. Acad. Sci. USA* **104**, 16793–16797.
17. Codelli, J. A., Baskin, J. M., Agard, N. J., and Bertozzi, C. R. (2008) Second-generation difluorinated cyclooctynes for copper-free click chemistry. *J. Am. Chem. Soc.* **130**, 11486–11493.
18. Ning, X. H., Guo, J., Wolfert, M. A., and Boons, G. J. (2008) Visualizing metabolically labeled glycoconjugates of living cells by copper-free and fast Husigen cycloadditions. *Angew. Chem. Int. Ed.* **47**, 2253–2255.
19. Laughlin, S. T., Baskin, J. M., Amacher, S. L., and Bertozzi, C. R. (2008) In vivo imaging of membrane-associated glycans in developing zebrafish. *Science* **320**, 664–667.
20. Devaraj, N. K., Weissleder, R., and Hilderbrand, S. A. (2008) Tetrazine-based cycloadditions: applications to pretargeted live cell imaging. *Bioconjug. Chem.* **19**, 2297–2299.
21. Blackman, M. L., Royzen, M., and Fox, J. M. (2008) Tetrazine ligation: fast bioconjugation based on inverse-electron-demand Diels-Alder reactivity. *J. Am. Chem. Soc.* **130**, 13518–13519.
22. Sampath, L., Kwon, S., Ke, S., Wang, W., Schiff, R., Mawad, M. F., and Sevick-Muraca, E. M. (2007) Dual-labeled trastuzumab-based imaging agent for the detection of human epidermal growth factor receptor 2 overexpression in breast cancer. *J. Nucl. Med.* **48**, 1501–1510.
23. Hicke, B. J., Stephens, A. W., Gould, T., Chang, Y.-F., Lynott, C. K., Heil, J., Borkowski, S., Hilger, C.-S., Cook, G., Warren, S., and Schmidt, P. G. (2006) Tumor targeting by an aptamer. *J. Nucl. Med.* **47**, 668–678.
24. Von Wallbrunn, A., Höltke, C., Zühlsdorf, M., Heindel, W., Schäfers, M., and Bremer, C. (2007) In vivo imaging of integrin a_vb_3 expression using fluorescence-mediated tomography. *Eur. J. Nucl. Med. Mol. Imaging* **34**, 745–754.
25. Garanger, E., Boturyn, D., Jin, Z., Dumy, P., Favrot, M.-C., and Coll, J.-L. (2005) New multifunctional molecular conjugate vector for targeting, imaging, and therapy of tumors. *Mol. Ther.* **12**, 1168–1175.
26. Jin, Z.-H., Josserand, V., Foillard, S., Boturyn, D., Dumy, P., Favrot, M.-C., and Coll, J.-L. (2007) In vivo optical imaging of integrin a_vb_3 in mice using multivalent or monovalent cRGD targeting vectors. *Mol. Cancer* **6**, 41.
27. Cheng, Z., Wu, Y., Xiong, Z., Gambhir, S. S., and Chen, X. (2005) Near-infrared fluorescent RGD peptides for optical imaging of integrin a_vb_3 expression in living mice. *Bioconjug. Chem.* **16**, 1433–1441.
28. Ke, S., Wen, X., Gurfinkel, M., Charnsangavej, C., Wallace, S., Sevick-Muraca, E. M., and Li, C. (2003) Near-infrared optical imaging of epidermal growth factor receptor in breast cancer xenografts. *Cancer Res.* **63**, 7870–7875.
29. Tung, C.-H., Lin, Y., Moon, W. K., and Weissleder, R. (2002) A receptor-targeted near-infrared fluorescence probe for in vivo tumor imaging. *Chembiochem* **3**, 784–786.
30. Weissleder, R., Kelly, K. A., Sun, E. Y., Shtatland, T., and Josephson, L. (2005) Cell-specific targeting of nanoparticles by multivalent attachment of small molecules. *Nat. Biotechnol.* **23**, 1418–1423.
31. Jaye, D. L., Geigerman, C. M., Fuller, R. E., Akyildiz, A., and Parkos, C. A. (2004) Direct fluorochrome labeling of phage display library clones for studying binding specificities: applications in flow cytometry and fluorescence microscopy. *J. Immunol. Methods.* **295**, 119–127.
32. Kelly, K. A., Bardeesy, N., Anbazhagan, R., Gurumurthy, S., Berger, J., Alencar, H., DePinho, R. A., Mahmood, U., and Weissleder, R. (2008) Targeted nanoparticles for imaging incipient pancreatic ductal adenocarcinoma. *PLOS Med.* **5**, 657–668.
33. Kelly, K. A., Setlur, S. R., Ross, R., Anbazhagan, R., Waterman, P., Rubin, M. A., and Weissleder, R. (2008) Detection of early prostate cancer using a hepsin-targeted imaging agent. *Cancer Res.* **68**, 2286–2291.
34. Hilderbrand, S. A., Kelly, K. A., Weissleder, R., and Tung, C.-H. (2005) Monofunctional near-infrared fluorochromes for imag-

ing applications. *Bioconjug Chem.* **16**, 1275–1281.
35. Weissleder, R., and Ntziachristos, V. (2003) Shedding light onto live molecular targets. *Nat. Med.* **9**, 123–128.
36. Mitchison, T. J. (1989) Polewards microtubule flux in the mitotic spindle: evidence from photoactivation of fluorescence. *J. Cell. Biol. 109*, 637–652.
37. Theriot, J. A., and Mitchison, T. J. (1991) Actin microfilament dynamics in locomoting cells. *Nature* **352**, 126–131.
38. Zhao, Y., Zheng, Q., Dakin, K., Xu, K., Martinez, M. L., and Li, W.-H. (2004) New caged coumarin fluorophores with extraordinary uncaging cross sections suitable for biological imaging applications. *J. Am. Chem. Soc.* **126**, 4653–4663.
39. Guo, Y.-M., Chen, S., Shetty, P., Zheng, G., Lin, R., and Li, W.-H. (2008) Imaging dynamic cell-cell junctional coupling in vivo using trojan-LAMP. *Nat. Methods* **5**, 835–841.
40. Flanagan, J. H., Jr., Khan, S. H., Menchen, S., Soper, S. A., and Hammer, R. P. (1997) Functionalized tricarbocyanine dyes as near-infrared fluorescent probes for biomolecules. *Bioconjug. Chem.* **8**, 751–756.
41. Narayanan, N., and Patonay, G. (1995) A new method for the synthesis of heptamethine cyanine dyes: synthesis of new near-infrared fluorescent labels. *J. Org. Chem.* **60**, 2391–2395.
42. Galande, A. K., Hilderbrand, S. A., Weissleder, R., and Tung, C.-H. (2006) Enzyme-targeted fluorescent imaging probes on a multiple antigenic peptide core. *J. Med. Chem.* **49**, 4715–4720.
43. Bruchez, M. J., Moronne, M., Gin, P., Weiss, S., and Alivisatos, A. P. (1998) Semiconductor nanocrystals as fluorescent biological labels. *Science* **281**, 2013–2016.
44. Wu, X., Liu, H., Liu, J., Haley, K. N., Treadway, J. A., Larson, J. P., Ge, N., Peale, F., and Bruchez, M. P. (2003) Immunofluorescent labeling of cancer marker Her2 and other cellular targets with semiconductor quantum Dots. *Nat. Biotechnol.* **21**, 41–46.
45. Derfus, A. M., Chan, W. C. W., and Bhatia, S. N. (2004) Probing the cytotoxicity of semiconductor quantum dots. *Nano Lett.* **4**, 11–18.
46. Mancini, M. C., Kairdolf, B. A., Smith, A. M., and Nie, S. (2008) Oxidative quenching and degradation of polymer-encapsulated quantum dots: new insights into the long-term fate and toxicity of nanocrystals in vivo. *J. Am. Chem. Soc.* **130**, 10836–10837.
47. Månsson, A., Sundberg, M., Balaz, M., Bunk, R., Nicholls, I. A., Olming, P., Tågerud, S., and Montelius, L. (2004) In vitro sliding of actin filaments labelled with single quantum dots. *Biochem. Biophys. Res. Commun.* **314**, 529–534.
48. Groc, L., Lafourcade, M., Heine, M., Renner, M., Racine, V., Sibarita, J.-B., Lounis, B., Choquet, D., and Cognet, L. (2007) Surface trafficking of neurotransmitter receptor: comparison between single-molecule/quantum dot strategies. *J. Neurosci.* **27**, 12433–12437.
49. Howarth, M., Liu, W., Puthenveetil, J., Zheng, Y., Marshall, L. F., Schmidt, M. M., Wittrup, K. D., Bawendi, M. G., and Ting, A. Y. (2008) Monovalent, reduced-size quantum dots for imaging receptors on living cells. *Nat. Methods* **5**, 397–399.
50. Miyawaki, A. (2008) Green fluorescent protein glows gold. *Cell* **135**, 987–990.
51. Shaner, N. C., Steinbach, P. A., and Tsien, R. Y. (2005) A guide to choosing fluorescent proteins. *Nat. Methods* **2**, 905–909.
52. Pakhomov, A. A., and Martynov, V. I. (2008) GFP family: structural insights into spectral tuning. *Chem. Biol.* **15**, 755–764.
53. Chalfie, M., Tu, Y., Euskirchen, G., Ward, W. W., and Prasher, D. C. (1994) Green fluorescent protein as a marker for gene expression. *Science* **263**, 802–805.
54. Weiner, O. D., Marganski, W. A., Wu, L. F., Altschuler, S. J., and Kirschner, M. W. (2007) An actin-based wave generator organizes cell motility. *PLOS Biol.* **5**, 2053–2063.
55. Weiner, O. D., Rentel, M. C., Ott, A., Brown, G. E., Jedrychowski, M., Yaffe, M. B., Gygi, S. P., Cantley, L. C., Bourne, H. R., and Kirschner, M. W. (2006) Hem-1 complexes are essential for Rac activation, actin polymerization, and myosin regulation during neutrophil chemotaxis. *PLOS Biol.* **4**, 0186–0199.
56. Sakaushi, S., Nishida, K., Minamikawa, H., Fukada, T., Oka, S., and Sugimoto, K. (2007) Live imaging of spindle pole disorganization in docetaxel-treated multicolor cells. *Biochem. Biophys. Res. Commun.* **357**, 655–660.
57. Fukada, T., Senda-Murata, K., Nishida, K., Sakaushi, S., Minamikawa, H., Dotsu, M., Oka, S., and Sugimoto, K. (2007) A multi-fluorescent MDA435 cell line for mitosis inhibitor studies: simultaneous visualization of chromatin, microtubules, and nuclear envelope in living cells. *Biosci. Biotechnol. Biochem.* **71**, 2603–2605.
58. De Wet, J. R., Wood, K. V., Helinski, D. R., and DeLuca, M. (1985) Cloning of fire-

fly luciferase cDNA and the expression of active luciferase in Escherichia coli. *Proc. Natl. Acad. Sci. USA.* **82**, 7870–7873.
59. Lorenz, W. W., McCann, R. O., Longiaru, M., and Cormier, M. J. (1991) Isolation and expression of a cDNA encoding *Renilla reniformis* luciferase. *Proc. Natl. Acad. Sci. U.S.A.* **88**, 4438–4442.
60. Stolz, U., Velez, S., Wood, K. V., Wood, M., and Feder, J. L. (2003) Darwinian natural selection for orange bioluminescent color in a Jamacian click beetle. *Proc. Natl. Acad. Sci. USA.* **100**, 14955–14959.
61. Wood, K. V., Lam, Y. A., and McElroy, W. D. (1989) Bioluminescent click beetles revisited. *J. Biolumin. Chemilumin.* **4**, 31–39.
62. Cohn, D. H., Mileham, A. J., Simon, M. I., and Nealson, K. H. (1985) Nucleotide sequence of the luxA gene of *Vibrio harveyi* and the complete amino acid sequence of the alpha subunit of bacterial luciferase. *J. Biol. Chem.* **260**, 6139–6146.
63. Johnston, T. C., Thompson, R. B., and Baldwin, T. O. (1986) Nucleotide sequence of the luxA gene of *Vibrio harveyi* and the complete amino acid sequence of the beta subunit of bacterial luciferase. *J. Biol. Chem.* **261**, 4805–4811.
64. Tung, C.-H., Bredow, S., Mahmood, U., and Weissleder, R. (1999) Preparation of a cathepsin D sensitive near-infrared fluorescence probe for imaging. *Bioconjug Chem.* **10**, 892–896.
65. Tung, C.-H., Mahmood, U., Bredow, S., and Weissleder, R. (2000) In vivo imaging of proteolytic enzyme activity using a novel molecular reporter. *Cancer Res.* **60**, 953–4958.
66. Bremer, C., Tung, C.-H., and Weissleder, R. (2001) In vivo molecular target assessment of matrix metalloproteinase inhibition. *Nat. Med.* **7**, 743–748.
67. Messerli, S. M., Prabhakar, S., Tang, Y., Shah, K., Cortes, M. L., Murthy, V., Weissleder, R., Breakefield, X. O., and Tung, C.-H. (2004) A novel method for imaging apoptosis using a caspase-1 near-infrared fluorescent probe. *Neoplasia* **6**, 95–105.
68. Jaffer, F. A., Kim, D.-E., Quinti, L., Tung, C.-H., Aikawa, E., Pande, A. N., Kohler, R. H., Shi, G.-P., Libby, P., and Weissleder, R. (2007) Optical visualization of cathepsin K activity in atherosclerosis with a novel, protease-activatable fluorescence sensor. *Circulation* **115**, 2292–2298.
69. Tanabe, H., Kumagai, N., Tsukahara, T., Ishiura, S., Kominami, E., Nishina, H., and Sugita, H. (1991) Changes of lysosomal proteinase activities and their expression in rat cultured keratinocytes during differentiation. *Biochim. Biophys. Acta, Mol. Cell Res.* **1094**, 281–287.
70. Selassie, C. D., Kapur, S., Verma, R. P., and Rosario, M. (2005) Cellular apoptosis and cytotoxicity of phenolic compounds: a quantitative structure-activity relationship study. *J. Med. Chem.* **48**, 7234–7242.
71. Liu, J., Bhlagat, M., Zhang, C., Diwu, Z., Hoyland, B., and Klaubert, D. H. (1999) Fluorescent molecular probes V: a sensitive caspase-3 substrate for fluorometric assays. *Bioorg. Med. Chem. Lett.* **9**, 3231–3236.
72. Tzougraki, C., Noula, C., Geiger, R., and Kokotos, G. (1994) Fluorogenic substrates containing 7-Amino-4-methyl-2-quinolinone for aminopeptidase M, chymotrypsin, elastase and trypsin, determination of enzyme activity. *Liebigs Ann. Chem.*, 365–368.
73. Rotman, B., Zderic, J. A., and Edelstein, M. (1963) Fluorogenic substrates for β-D-dalactosidases and phosphatases derived from fluorescein (3,6-dihydroxyfluoran) and its monomethyl ether. *Proc. Natl. Acad. Sci. U.S.A.* **50**, 1–6.
74. Takahashi, A., Camacho, P., Lechleiter, J. D., and Herman, B. (1999) Measurement of intracellular calcium. *Physiol. Rev.* **79**, 1089–1125.
75. Paredes, R. M., Etzler, J. C., Watts, L. T., Zheng, W., and Lechleiter, J. D. (2008) Chemical calcium indicators. *Methods* **46**, 143–151.
76. Heinonen, E., and Akerman, K. E. (1987) Intracellular free magnesium in synaptosomes measured with entrapped eriochrome blue. *Biochim. Biophys. Acta Biomembr.* **898**, 331–337.
77. Gryzkiewicz, G., Poenie, M., and Tsien, R. Y. (1985) A new generation of Ca^{2+} indicators with greatly improved fluorescence properties. *J. Biol. Chem.* **260**, 3440–3450.
78. Tsien, R. Y. (1980) New calcium indicators and buffers with high selectivity against magnesium and protons: design, synthesis, and properties of prototype structures. *Biochemistry* **19**, 2396–2404.
79. Domaille, D. W., Que, E. L., and Chang, C. J. (2008) Synthetic fluorescent sensors for studying the cell biology of metals. *Nat. Chem. Biol.* **4**, 168–175.
80. Kikuchi, K., Komatsu, K., and Nagano, T. (2004) Sensing for cellular application. *Curr. Opin. Chem. Biol.* **8**, 182–191.
81. Thompson, R. B. (2005) Studying zinc biology with fluorescence: ain't we got fun? *Curr. Opin. Chem. Biol.* **9**, 526–532.
82. Walkup, G. K., Burdette, S. C., and Lippard, S. J. (2000) A new cell-permeable fluorescent

probe for Zn(II). *J. Am. Chem. Soc.* **122**, 5644–5645.
83. Chang, C. J., Nolan, E. M., Jaworski, J., Burdette, S. C., Sheng, M., and Lippard, S. J. (2004) Bright fluorescent chemosensor platforms for imaging endogenous pools of neuronal zinc. *Chem. Biol.* **11**, 203–210.
84. Woodroofe, C. C., Masalha, R., Barnes, K. R., Fredrickson, C. J., and Lippard, S. J. (2004) Membrane-permeable and -impermeable sensors of the zinpyr family and their application to imaging of hippocampal zinc in vivo. *Chem. Biol.* **11**, 1659–1666.
85. Nolan, E. M., Burdette, S. C., Harvey, J. H., Hilderbrand, S. A., and Lippard, S. J. (2004) Synthesis and characterization of zinc sensors based on a monosubstituted fluorescein platform. *Inorg. Chem.* **43**, 2624–2635.
86. Nolan, E. M., Ryu, J. W., Jaworski, J., Feazell, R. P., Sheng, M., and Lippard, S. J. (2006) Zinspy sensors with enhanced dynamic range for imaging neuronal cell zinc uptake and mobilization. *J. Am. Chem. Soc.* **128**, 15517–15528.
87. Hirano, T., Kikuchi, K., Urano, Y., Higuchi, T., and Nagano, T. (2000) Highly zinc-selective fluorescent sensor molecules suitable for biological applications. *J. Am. Chem. Soc.* **122**, 12399–12400.
88. Hirano, T., Kikuchi, K., Urano, Y., and Nagano, T. (2002) Improvement and biological applications of fluorescent probes for ainc, ZnAFs. *J. Am. Chem. Soc.* **124**, 6555–6562.
89. Takeda, A., Nakajima, S., Fuke, S., Sakurada, N., Minami, A., and Oku, N. (2006) Zinc release from schaffer collaterals and its significance. *Brain Res. Bull.* **68**, 442–447.
90. Komatsu, K., Kikuchi, K., Kojima, H., Urano, Y., and Nagano, T. (2005) Selective zinc sensor molecules with various affinities for Zn^{2+}, revealing dynamics and regional distribution of synaptically released Zn^{2+} in hippocampal slices. *J. Am. Chem. Soc.* **127**, 10197–10204.
91. Gee, K. R., Zhou, Z. L., Ton-That, D., Sensi, S. L., and Weiss, J. H. (2002) Measuring zinc in living cells. A new generation of sensitive and selective fluorescent probes. *Cell Calcium* **31**, 245–251.
92. MacDiarmid, C. W., Milanick, M. A., and Eide, D. J. (2003) Induction of the ZRC1 metal tolerance gene in zinc-limited yeast confers resistance to zinc shock. *J. Biol. Chem.* **278**, 15065–15072.
93. Chang, C. J., Jaworski, J., Nolan, E. M., Sheng, M., and Lippard, S. J. (2004) A tautomeric zinc sensor for ratiometric fluorescence imaging: application to nitric oxide-induced release of intracellular zinc. *Proc. Natl. Acad. Sci. U.S.A.* **101**, 1129–1134.
94. Kiyose, K., Kojima, H., Urano, Y., and Nagano, T. (2006) Development of a ratiometric fluorescent zinc ion probe in near-infrared region, based on tricarbocyanine chromophore. *J. Am. Chem. Soc.* **128**, 6548–6549.
95. Kellum, J. A., Song, M., and Li, J. (2004) Extracellular acidosis and the immune response: clinical and physiologic implications. *Crit. Care* **8**, 331–336.
96. Coakley, R. D., Grubb, B. R., Paradiso, A. M., Gatzy, J. T., Johnson, L. G., Kreda, S. M., O'Neal, W. K., and Boucher, R. C. (2003) Abnormal surface liquid pH regulation by cultured cystic fibrosis bronchial epithelium. *Proc. Natl. Acad. Sci. USA* **100**, 16083–16088.
97. Gillies, R. J., Raghunand, N., Garcia-Martin, M. L., and Gatenby, R. A. (2004) pH Imaging. *IEEE Eng. Med. Biol. Mag.* **23**, 57–64.
98. Gillies, R. J., Schornack, P. A., Secomb, T. W., and Raghunand, N. (1999) Causes and effects of heterogenous perfusion in tumors. *Neoplasia* **1**, 197–207.
99. Heiple, J. M., and Taylor, D. L. (1980) Intracellular pH in single motile cells. *J. Cell. Biol.* **86**, 885–890.
100. Khodorov, B., Valkina, O., and Turovetsky, V. (1994) Mechanisms of stimulus-evoked intracellular acidification in frog nerve fibers. *FEBS Lett.* **341**, 125–127.
101. Burns, A., Sengupta, P., Zedayko, T., Baird, B., and Weisner, U. (2006) Core/shell fluorescent silica nanoparticles for chemical sensing: towards single cell particle laboratories. *Small* **2**, 723–726.
102. Rink, T. J., Tsien, R. Y., and Pozzan, T. (1982) Cytoplasmic pH and free Mg^{2+} in lymphocytes. *J. Cell. Biol.* **95**, 189–196.
103. Whitaker, J. E., Haughland, R. P., and Prendergast, F. G. (1991) Spectral and photophysical studies of benz[c]xanthene dyes: dual emission pH sensors. *Anal. Biochem.* **194**, 330–344.
104. Bassnett, S., Reinisch, L., and Bebee, D. C. (1990) Intracellular pH measurement using single excitation dual emission fluorescence ratios. *Am. J. Phys. Cell Physiol.* **258**, 171–178.
105. Urano, Y., Asanuma, D., Hama, Y., Koyama, Y., Barrett, T., Kamiya, M., Nagano, T., Watanabe, T., Hasegawa, A., Choyke, P. L., and Kobayashi, H. (2008) Selective molecular imaging of viable cancer cells with pH-activatable fluorescent probes. *Nat. Med.* **15**, 104–109.

106. Adie, E. J., Kalinka, S., Smith, L., Francis, M. J., Marenghi, A., Cooper, M. E., Briggs, M., Michael, N. P., Milligan, G., and Game, S. (2002) A pH-sensitive fluor, CypHer5, used to monitor agonist-induced G protein-coupled receptor internalization in live cells. *BioTechniques* **33**, 1152–1157.
107. Cooper, M. E., Gregory, S., Adie, E., and Kalinka, S. (2002) pH-Sensitive cyanine dyes for biological applications. *J. Fluoresc.* **12**, 425–429.
108. Hilderbrand, S. A., and Weissleder, R. (2007) Optimized pH-responsive cyanine fluorochromes for detection of acidic environments. *Chem. Commun.*, 2747–2749.
109. Hilderbrand, S. A., Kelly, K. A., Niedre, M., and Weissleder, R. (2008) Near infrared fluorescence-based bacteriophage particles for ratiometric pH imaging. *Bioconjug. Chem.* **19**, 1635–1639.
110. Minta, A., and Tsien, R. Y. (1989) Fluorescent indicators for cytosolic sodium. *J. Biol. Chem.* **264**, 19449–19457.
111. Meuwis, K., Boens, N., De Schryver, F. C., Gallay, J., and Vincent, M. (1995) Photophysics of the fluorescent K^+ indicator PBFI. *Biophys. J.* **68**, 2469–2473.
112. Valentine, J. S., and Hart, P. J. (2003) Misfolded CuZnSOD and amyotrophic lateral sclerosis. *Proc. Natl. Acad. Sci. U.S.A.* **100**, 3617–3622.
113. Barnham, K. J., Masters, C. L., and Bush, A. I. (2004) Neurodegenerative diseases and oxidative stress. *Nat. Rev. Drug Discov.* **3**, 205–214.
114. Yang, L. C., McRae, R., Henary, M. M., Patel, R., Lai, B., Vogt, S., and Fahrni, C. J. (2005) Imaging of the intracellular topography of copper with a fluorescent sensor and by synchrottron X-ray fluorescence microscopy. *Proc. Natl. Acad. Sci. U.S.A.* **102**, 11178–11184.
115. Zeng, L., Miller, E. W., Domaille, D. W., and Chang, C. J. (2006) A selective turn-on fluorescent sensor for imaging copper in living cells. *J. Am. Chem. Soc.* **128**, 10–11.
116. Miller, E. W., Zeng, L., Domaille, D. W., and Chang, C. J. (2006) Preparation and use of coppersensor-1, a synthetic fluorophore for live-cell copper imaging. *Nat. Protoc.* **1**, 824–827.
117. Hua, J., and Wang, Y. G. (2005) A highly selective and sensitive fluorescent chemosensor for Fe(III) in physiological aqueous solution. *Chem. Lett.* **34**, 98–99.
118. Xiang, Y., and Tong, A. (2006) A new rhodamine-based chemosensor exhibiting selective Fe(III)-amplified fluorescence. *Org. Lett.* **8**, 1549–1552.
119. Zhang, M., Gao, Y., Li, M., Yu, M., Li, F., Li, L., Zhu, M., Zhang, J., Yi, T., and Huang, C. (2007) A selective turn-on fluorescent sensor for FeIII and application to bioimaging. *Tet. Lett.* **48**, 3709–3712.
120. Lin, W., Yuan, L., Feng, J., and Cao, X. (2008) A fluorescence-enhanced chemodosimeter for Fe^{3+} based on hydrolysis of a bis(coumarinyl) schiff base. *Eur. J. Org. Chem.*, 2689–2692.
121. Setsukinai, K.-I., Urano, Y., Kakinuma, K., Majima, H. J., and Nagano, T. (2003) Development of novel fluorescence probes that can reliably detect reactive oxygen species and distinguish specific species. *J. Biol. Chem.* **278**, 3170–3175.
122. Lim, M. H., and Lippard, S. J. (2007) Metal-based turn-on fluorescent probes for sensing nitric oxide. *Acc. Chem. Res.* **40**, 41–51.
123. Nagano, T., and Yoshimura, T. (2002) Bioimaging of nitric oxide. *Chem. Rev.* **102**, 1235–1269.
124. Nakatsubo, N., Kojima, H., Sakurai, K., Kikuchi, K., Nagoshi, H., Hirata, Y., Akaike, T., Maeda, H., Urano, Y., Higuchi, T., and Nagano, T. (1998) Improved nitric oxide detection using 2,3-diaminonaphthalene and its application to the evaluation of novel nitric oxide synthase inhibitiors. *Biol. Pharm. Bull.* **21**, 1247–1250.
125. Kojima, H., Nakatsubo, N., Kikuchi, K., Kawahara, S., Kirino, Y., Nagoshi, H., Hirata, Y., and Nagano, T. (1998) Detection and imaging of nitric oxide with novel fluorescent indicators: diaminofluoresceins. *Anal. Chem.* **70**, 2446–2453.
126. Gabe, Y., Urano, Y., Kikuchi, K., Kojima, H., and Nagano, T. (2004) Highly sensitive fluorescence probes for nitric oxide based on boron dipyrromethane chromophore-rational design of potentially useful bioimaging fluorescence probe. *J. Am. Chem. Soc.* **126**, 3357–3367.
127. Kojima, H., Hirotani, M., Nakatsubo, N., Kikuchi, K., Urano, Y., Higuchi, T., Hirata, Y., and Nagano, T. (2001) Bioimaging of nitric oxide with fluorescent indicators based on the rhodamine chromophore. *Anal. Chem.* **73**, 1967–1973.
128. Sasaki, E., Kojima, H., Nishimatsu, H., Urano, Y., Kikuchi, K., Hirata, Y., and Nagano, T. (2005) Highly sensitive near-infrared fluorescent probes for nitric oxide and their application to isolated organs. *J. Am. Chem. Soc.* **127**, 3684–3685.
129. Lim, M. H., Xu, D., and Lippard, S. J. (2006) Visualization of nitric oxide in living cells by a copper-based fluorescent probe. *Nat. Chem. Biol.* **2**, 375–380.

130. Lim, M. H., Wong, B. A., Pitcock, W. H., Mokshagundam, D., Baik, M.-H., and Lippard, S. J. (2006) Direct nitric oxide detection in aqueous solution by copper(II) fluorescein complexes. *J. Am. Chem. Soc.* **128**, 14364–14373.
131. Maeda, H., Fukuyasu, Y., Yoshida, S., Fukuda, M., Saeki, K., Matsuno, H., Yamauchi, Y., Yoshida, K., Hirata, K., and Miyamoto, K. (2004) Fluorescent probes for hydrogen peroxide based on a nonoxidative mechanism. *Angew. Chem., Int. Ed.* **43**, 2389–2391.
132. Maeda, H., Yamamoto, K., Nomura, Y., Kohno, I., Hafsi, L., Ueda, N., Yoshida, S., Fukuda, M., Fukuyasu, Y., Yamauchi, Y., and Itoh, N. (2005) A design of fluorescent probes for superoxide based on a nonredox rechanism. *J. Am. Chem. Soc.* **127**, 68–69.
133. Xu, K., Tang, B., Huang, H., Yang, G., Chen, Z., Li, P., and An, L. (2005) Strong red fluorescent probes suitable for detecting hydrogen peroxide generated by mice peritoneal macrophages. *Chem. Commun.*, 5974–5976.
134. Chang, M. C. Y., Pralle, A., Isacoff, E. Y., and Chang, C. J. (2004) A selective, cell permeable optical probe for hydrogen peroxide in living cells. *J. Am. Chem. Soc.* **126**, 15392–15393.
135. Miller, E. W., Albers, A. E., Pralle, A., Isacoff, E. Y., and Chang, C. J. (2005) Boronate-based fluorescent probes for imaging cellular hydrogen peroxide. *J. Am. Chem. Soc.* **127**, 16652–16659.
136. Miller, E. W., Tulyathan, O., Isacoff, E. Y., and Chang, C. J. (2007) Molecular imaging of hydrogen peroxide produced for cell signaling. *Nat. Chem. Biol.* **3**, 263–267.
137. Albers, A. E., Dickinson, B. C., Miller, E. W., and Chang, C. J. (2008) A red-emitting naphthofluorescein-based fluorescent probe for selective detection of hydrogen peroxide in living cells. *Bioorg. Med. Chem. Lett.* **18**, 5948–5950.
138. Lee, D., Khaja, S., Velasquez-Castano, J. C., Dasari, M., Sun, C., Petros, J., Taylor, W. R., and Murthy, N. (2007) In vivo imaging of hydrogen peroxide with chemiluminescent nanoparticles. *Nat. Mater.* **6**, 765–769.
139. Shepherd, J., Hilderbrand, S. A., Waterman, P., Heinecke, J. W., Weissleder, R., and Libby, P. (2007) A fluorescent probe for the detection of myleoperoxidase activity in atherosclerosis-associated macrophages. *Chem. Biol.* **14**, 1221–1231.
140. Kundu, K., Knight, S. F., Willett, N., Lee, S., Taylor, W. R., and Murthy, N. (2009) Hydrocyanines: a class of fluorescent sensors that can image reactive oxygen species in cell culture, tissue, and in vivo. *Angew. Chem., Int. Ed.* **48**, 299–303.
141. Yang, D., Wang, H.-L., Sun, Z.-N., Chung, N.-W., and Shen, J.-G. (2006) A highly selective fluorescent probe for the detection and imaging of peroxynitrite in living cells. *J. Am. Chem. Soc.* **128**, 6004–6005.
142. Seshadri, S., Beiser, A., Selhub, J., Jacques, P. F., Rosenberg, I. H., D'Agostino, R. B., Wilson, P. W. F., and Wolfe, P. A. (2002) Plasma homocysteine as a risk factor for dementia and alzheimer's disease. *New Engl. J. Med.* **346**, 476–483.
143. Refsum, H., and Ueland, P. M. (1998) Homocysteine and cardiovascular disease. *Annu. Rev. Med.* **49**, 31–62.
144. Duan, L., Xu, Y., Qian, X., Wang, F., Liu, J., and Cheng, T. (2008) Highly selective fluorescent chemosensor with red shift for cysteine in buffer solution and its bioimage: symmetrical naphthalimide aldehyde. *Tet. Lett.* **49**, 6624–6627.
145. Lin, W., Long, L., Yuan, L., Cao, Z., Chen, B., and Tan, W. (2008) A ratiometric fluorescent probe for cysteine and homocysteine displaying a large emission shift. *Org. Lett.* **10**, 5577–5580.
146. Bouffard, J., Kim, Y., Swager, T. M., Weissleder, R., and Hilderbrand, S. A. (2008) A highly selective fluorescent probe for thiol bioimaging. *Org. Lett.* **10**, 37–40.
147. Jiang, W., Fu, W., Fan, H., Ho, J., and Wang, W. (2007) A highly selective fluorescent probe for thiophenols. *Angew. Chem., Int. Ed.* **46**, 8445–8448.